

**NOTE:****Docking-Guided 3D-QSAR Studies of 4-Aminoquinoline-1,3,5-triazines as Inhibitors for *Plasmodium falciparum* Dihydrofolate Reductase**Radite Yogaswara<sup>1</sup>, Maria Ludya Pulung<sup>2</sup>, Sri Hartati Yuliani<sup>3</sup>, and Enade Perdana Istyastono<sup>3,\*</sup><sup>1</sup>Department of Chemistry Education, Faculty of Education and Teachers Training, University of Papua, Manokwari 98311, Indonesia<sup>2</sup>Department of Chemistry, Faculty of Mathematics and Natural Science, University of Papua, Manokwari 98311, Indonesia<sup>3</sup>Faculty of Pharmacy, Sanata Dharma University, Paingan, Maguwoharjo, Depok, Sleman, Yogyakarta 55282, Indonesia**\* Corresponding author:**

email: enade@usd.ac.id

Received: October 17, 2019

Accepted: March 26, 2020

DOI: 10.22146/ijc.50674

**Abstract:** Mutations in *Plasmodium falciparum* dihydrofolate reductase (PfDHFR), together with other mutations, hinder malaria elimination in Southeast Asia due to multiple drug resistance. In this article, molecular docking-guided three-dimensional (3D) quantitative structure-activity relationship (QSAR) analysis of 4-aminoquinoline-1,3,5-triazines as inhibitors for the wild-type (WT) PfDHFR to identify the molecular determinants of the inhibitors binding are presented. Compounds 4-aminoquinoline-1,3,5-triazines were reported promising to be developed as the non-resistant drugs. The 3D-QSAR analysis resulted in the best model with the  $R^2$  and  $Q^2$  values of 0.881 and 0.773, respectively. By correlating the molecular interaction fields (MIFs) of the best model to the docking pose employed to guide the 3D-QSAR analysis,  $S^{108}$  residue of the WT-PfDHFR was unfortunately recognized as one of the molecular determinants. Since the  $S^{108}$  residue is one of the mutation points of the PfDHFR mutants, the subsequent design strategy should modify the morpholine moiety to avoid the interaction with the  $S^{108}$  residue of the WT-PfDHFR.

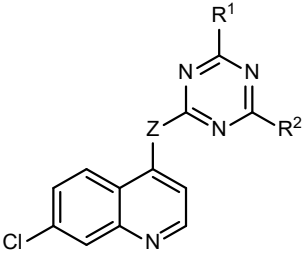
**Keywords:** *Plasmodium falciparum* dihydrofolate reductase; 3D-QSAR; molecular docking; multiple drug resistance

**■ INTRODUCTION**

The cases of malaria globally showed a significant decreased in 2018 (228 million cases) compared to those in 2010 (252 million cases) and in 2017 (231 million cases) [1]. However, the number is still considerably high, and the same report [1] also presents high failure rates of treatment with artesunate-sulfadoxine-pyrimethamine for *Plasmodium falciparum*, due to drug resistance. This drug resistance is highly related to the presence of some *Plasmodium falciparum* dihydrofolate reductase (PfDHFR) mutants [2], since PfDHFR is the drug target of pyrimethamine [2-3]. On the other hand, the attempts to design and synthesize non-resistant drugs against PfDHFR and its mutants have resulted in some promising scaffolds, one of which is the 4-aminoquinoline-1,3,5-

triazines [4]. Some 4-aminoquinoline-1,3,5-triazines and their biological activities against WT-PfDHFR are presented in Table 1.

Computer-aided techniques have been employed to pinpoint the molecular determinants of ligands binding [5-7]. Molecular docking-guided three-dimensional (3D) quantitative structure-activity relationship (QSAR) analysis of some clobenpropit derivatives as ligands for histamine H4 receptor successfully identify the molecular determinants of ligand bindings, which were verified by site-directed mutagenesis studies and molecular dynamics simulations [5]. Equipped with the information of the molecular determinants of ligands binding, subsequent successful structure-based virtual screening (SBVS) campaigns could

**Table 1.** Structures and biological activities of some 4-aminoquinoline-1,3,5-triazines as inhibitors for WT-PfDHFR [4-5]


Compound	Z	R <sup>1</sup>	R <sup>2</sup>	IC <sub>50</sub> (μg/mL)
1	1,2-Ethylenediamine	Piperidine	3-Aminopropylmorpholine	7.79
2	1,2-Ethylenediamine	Piperidine	<i>N,N</i> -Diethylethylenediamine	10.15
3	1,2-Ethylenediamine	Piperidine	<i>N,N</i> -Dimethylethylenediamine	13.34
4	1,2-Ethylenediamine	Piperidine	<i>N</i> -Methylpiperazine	9.10
5	1,2-Ethylenediamine	Morpholine	3-Aminopropylmorpholine	8.58
6	1,2-Ethylenediamine	Morpholine	<i>N,N</i> -Diethylethylenediamine	9.42
7	1,2-Ethylenediamine	Morpholine	<i>N,N</i> -Dimethylethylenediamine	8.10
8	1,2-Ethylenediamine	Morpholine	<i>N</i> -Methylpiperazine	6.19
9	1,2-Ethylenediamine	Morpholine	2-Aminoethylmorpholine	17.16
10	1,3-Propanediamine	Piperidine	3-Aminopropylmorpholine	7.54
11	1,3-Propanediamine	Piperidine	<i>N,N</i> -Diethylethylenediamine	7.45
12	1,3-Propanediamine	Piperidine	<i>N,N</i> -Dimethylethylenediamine	8.19
13	1,3-Propanediamine	Piperidine	<i>N</i> -Methylpiperazine	7.45
14	1,3-Propanediamine	Morpholine	3-Aminopropylmorpholine	8.60
15	1,3-Propanediamine	Morpholine	<i>N,N</i> -Diethylethylenediamine	10.64
16	1,3-Propanediamine	Morpholine	<i>N,N</i> -Dimethylethylenediamine	7.94
17	1,3-Propanediamine	Morpholine	<i>N</i> -Methylpiperazine	8.55
18	1,3-Propanediamine	Morpholine	2-Aminoethylmorpholine	8.72

identify verified hits for histamine H4 receptor with  $K_i$  values in the nanomolar range [8]. Another strategy was combining retrospective SBVS campaigns with PyPLIF [9-10] and RPART [11]. However, the strategy required a large dataset of active compounds and their decoys [7,12-13]. Since we do not have the luxury of the large dataset, the first strategy by combining molecular docking and 3D-QSAR analysis was of considerable interest.

The research presented in this article aimed to virtually identify molecular determinants in the PfDHFR-inhibitor bindings and examined if the molecular determinants were one of the common mutations in PfDHFR, which could lead to resistance [2]. Similar techniques to Istyastono et al. [5] were employed to pinpoint the molecular determinants. Since one of the mutation points was unfortunately identified as a molecular determinant of the inhibitors binding, the

compounds in Table 1 are very unlikely to be developed as non-resistant malaria drugs.

## ■ COMPUTATIONAL DETAILS

### Materials

The compounds and their biological activities in Table 1 [4-6] were used in the 3D-QSAR analysis. Computation for the 3D-QSAR studies was performed in a machine with Intel<sup>(R)</sup> Core™ i7-4770S PC @ 3.10GHz CPU as the processor, 12 GB of RAM, and 1 TB of hard disk drive (HDD). The main material for the docking simulations was the crystal structure of the Wild-type PfDHFR complexed with pyrimethamine (PDB:3QGT) [3]. Computation for the docking simulations was performed in the same machine used by Yuniarti et al. [14].

## Software

The 3D-QSAR studies were performed by employing Open3DQSAR software [15]. In this research, the Open3DQSAR software employed some plugins, i.e., OpenBabel for Open3DTools, GRID from molecular discovery, Gnuplot 4.6.5, Pymol 1.7.1, and Python 2.7.6. The molecular docking simulations were mainly performed by employing PLANTS docking software version 1.2 [16-17]. Additional software used during the preparation of the docking input files and the analysis of the output files were SPORES version 1.3 [18], Open Babel [19], fconv [20], and Pymol 2.3.4 [21].

## Procedure

### Molecular docking simulations

The chain A of PDB:3QGT was extracted from the 3QGT.pdb and saved as 3QGT\_A.pdb. The later was then prepared using the module *splitpdb* in SPORES1.3 resulted in output files *protein.mol2* for the virtual protein target in the next simulations and *ligand\_CP6609\_0.mol2* as the co-crystal ligand. For validation, the co-crystal ligand *ligand\_CP6609\_0.mol2* was docked 1000 times using PLANTS1.2 with the configuration file similar to the one used by Riswanto et al. [13]. The binding site definition was changed in this research to adapt the coordinate the co-crystal ligand *ligand\_CP6609\_0.mol2* in the *protein.mol2*. The docking protocol was acceptable if more than 95% of docking poses have root-mean-square deviation (RMSD) values of less than 2.0 Å. By employing the validated docking protocol, compound **8** was docked 1000 times, and the pose with the best ChemPLP score as the docking score was selected as the reference pose for the 3D-QSAR analysis. Compound **8** was selected since it showed the best IC<sub>50</sub> value (Table 1).

### 3D-QSAR analysis

All molecules in Table 1 were superposed to the best docking pose of compound **8** as the alignment template. The 18 aligned molecules were then placed in a 3D cubic lattice with 2.0 Å spacing outside the aligned poses. The steric and electrostatic interaction energies were calculated for each molecule at 2.0 Å grid point. The energy cut off was set between -40.0 to 40.0 kcal/mol. Regression analysis was performed by using the Partial Least Squares (PLS)

technique. The smart region definition (SRD) uninformative and iterative variable elimination (UVE/IVE) PLS method were used for data-noise reduction [15]. The internal validation procedures were performed by using leave-many-out cross-validation. The 3D-QSAR models were considered as acceptable if the Q<sup>2</sup> values are greater than 0.5, while the best 3D-QSAR was selected by evaluating the R<sup>2</sup> values. The model with the highest R<sup>2</sup> value was selected as the best model.

## RESULTS AND DISCUSSION

Aimed to identify the molecular determinants in WT-PfDHFR-inhibitor bindings, a similar strategy introduced by Istyastono et al. [6] was performed. The results of the 3D-QSAR analysis are presented in Table 2. The MIFs of model 5 (Table 2) as the best model is depicted in Fig. 1(a), while the best docking pose of compound **8** is presented in Fig. 1(b) to assist the visual inspection.

The validation of the docking protocol resulted in RMSD values ≤ 2.0 Å for 996 poses out of 1000 re-docking simulations. Thus, the protocol was acceptable to be used further to dock compound **8**, which was selected due to its highest activity as an inhibitor for PfDHFR (Table 1) [4]. The best docking pose of compound **8** resulted from the docking number 475 with a ChemPLP value of -99.099. Similar to [5], the pose was then used as the reference pose for the 3D-QSAR analysis. The R<sup>2</sup> value (0.762) of model 5 (Table 2) was slightly better than the QSAR model with R<sup>2</sup> value of 0.69 presented by Hadni et al. [6]. Nevertheless, the Q<sup>2</sup> value (0.761) was not as good as the QSAR model with Q<sup>2</sup> value of 0.81 presented by Hadni et al. [6]. Notably, the statistical significance values of model 5 (Table 2) as the best model resulted from the 3D-QSAR analysis are considered as acceptable.

**Table 2.** Results of the 3D-QSAR analysis

No.	3D-QSAR Models	R <sup>2</sup>	Q <sup>2</sup>
1.	1	0.121	0.117
2.	2	0.420	0.410
3.	3	0.623	0.642
4.	4	0.711	0.710
5.	5	0.762	0.761

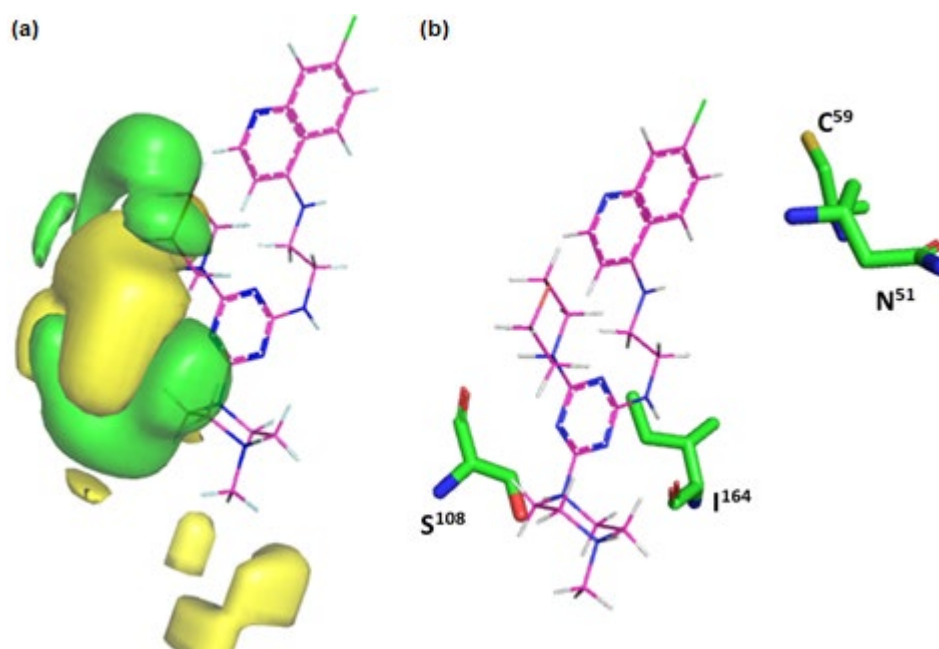


**Fig 1.** (a) The MIFs (the favorable steric fields are depicted in green; the unfavorable steric fields are depicted in yellow) of the best model with the pose of compound **8** (shown in line mode with carbon atoms in magenta) as the reference pose; and (b) The best pose of compound **8** in the binding pocket (shown in stick mode, with carbon atoms in green). Only mutated residues in double and quadruple mutants of PfDHFR are shown. Oxygen, nitrogen, hydrogen, and chlorine atoms are depicted in red, blue, white, and light green, respectively. The pictures were prepared using Pymol 2.3.4 [20]

Visual inspection to correlate the MIFs resulted from the 3D-QSAR analysis to the binding pocket residues (Fig. 1) identified S<sup>108</sup> as one of the molecular determinants of the PfDHFR-inhibitor bindings in this compound series (Table 1). There are two mutation points C<sup>59</sup>R/S<sup>108</sup>N in the PfDHFR double mutant, and four mutation points N<sup>51</sup>I/C<sup>59</sup>R/S<sup>108</sup>N/I<sup>164</sup>L in the PfDHFR quadruple mutant [2-3]. Thus, the identification of S<sup>108</sup> as one of the molecular determinants indicates the high probability of compounds presented in Table 1 to develop resistances against both PfDHFR mutants. Equipped with this information, a new strategy should be developed to design non-resistant malaria drugs. These results also present the complexity of designing non-resistant malaria drugs.

The MIFs resulted in the 3D-QSAR analysis indicated that non-polar interactions between the compound series played an important role in their activity as WT-PfDHFR inhibitors (Fig. 1(a)). Since the MIFs overlapped with the S<sup>108</sup> residue (Fig. 1), it is not trivial to design a non-resistant drug [6]. The subsequent design

should avoid the interactions with the potential mutation points. Visual inspection of the binding of compound **8** to PfDHFR shows possibilities to explore R<sup>2</sup> part of the substitution with polar moieties and reduce the size of the R<sup>1</sup> part. This new design strategy enables the increase of polar interactions with the outer part of the PfDHFR while reducing the probability of having steric interactions with S<sup>108</sup>. The compounds designed with this strategy could be developed as non-resistant malaria drugs. Molecular dynamics simulations could be employed to examine the stability and the binding affinity of such compounds to the WT-PfDHFR and its mutants [22-23].

## ■ CONCLUSION

Molecular docking-guided 3D-QSAR studies identified S<sup>108</sup> as one of the molecular determinants of the PfDHFR-inhibitor bindings of the compound series presented in Table 1. This indicates that the compounds could develop resistances in the PfDHFR mutants. A new design strategy that enables the increase of polar

interactions with the outer part of the PfDHFR while reducing the probability of having steric interactions with S<sup>108</sup> should be adapted.

## ■ ACKNOWLEDGMENTS

This project has received funding from the Indonesian National Research and Innovation Agency under grant agreement No. 198/SP2H/AMD/LT/DRPM/2020.

## ■ REFERENCES

- [1] World Health Organization, 2019, *World Malaria Report 2019*, Geneva.
- [2] Yuvaniyama, J., Chitnumsub, P., Kamchonwongpaisan, S., Vanichtanankul, J., Sirawaraporn, W., Taylor, P., Walkinshaw, M.D., and Yuthavong, Y., 2003, Insights into antifolate resistance from malarial DHFR-TS structures, *Nat. Struct. Biol.*, 10 (5), 357–365.
- [3] Vanichtanankul, J., Taweechai, S., Yuvaniyama, J., Vilaivan, T., Chitnumsub, P., Kamchonwongpaisan, S., and Yuthavong, Y., 2011, Trypanosomal dihydrofolate reductase reveals natural antifolate resistance, *ACS Chem. Biol.*, 6 (9), 905–911.
- [4] Sunduru, N., Sharma, M., Srivastava, K., Rajakumar, S., Puri, S.K., Saxena, J.K., and Chauhan, P.M.S., 2009, Synthesis of oxalamide and triazine derivatives as a novel class of hybrid 4-aminoquinoline with potent antiplasmodial activity, *Bioorg. Med. Chem.*, 17 (17), 6451–6462.
- [5] Istyastono, E.P., Nijmeijer, S., Lim, H.D., van de Stolpe, A., Roumen, L., Kooistra, A.J., Vischer, H.F., de Esch, I.J.P., Leurs, R., and de Graaf, C., 2011, Molecular determinants of ligand binding modes in the histamine H<sub>4</sub> receptor: Linking ligand-based three-dimensional quantitative structure–activity relationship (3D-QSAR) models to in silico guided receptor mutagenesis studies, *J. Med. Chem.*, 54 (23), 8136–8147.
- [6] Hadni, H., Mazigh, M., Charif, E., Bouayad, A., and Elhallaoui, M., 2018, Molecular modeling of antimalarial agents by 3D-QSAR study and molecular docking of two hybrids 4-Aminoquinoline-1,3,5-triazine and 4-Aminoquinoline-oxalamide derivatives with the receptor protein in its both wild and mutant types, *Biochem. Res. Int.*, 2018, 8639173.
- [7] Istyastono, E.P., Yuniarti, N., Hariono, M., Yuliani, S.H., and Riswanto, F.D.O., 2017, Binary quantitative structure-activity relationship analysis in retrospective structure based virtual screening campaigns targeting estrogen receptor alpha, *Asian J. Pharm. Clin. Res.*, 10 (12), 206–211.
- [8] Istyastono, E.P., Kooistra, A.J., Vischer, H., Kuijter, M., Roumen, L., Nijmeijer, S., Smits, R., de Esch, I., Leurs, R., and de Graaf, C., 2015, Structure-based virtual screening for fragment-like ligands of the G protein-coupled histamine H<sub>4</sub> receptor., *Med. Chem. Commun.*, 6 (6), 1003–1017.
- [9] Radifar, M., Yuniarti, N., and Istyastono, E.P., 2013, PyPLIF: Python-based protein-ligand interaction fingerprinting, *Bioinformatics*, 9 (6), 325–328.
- [10] Radifar, M., Yuniarti, N., and Istyastono, E.P., 2013, PyPLIF-assisted redocking indomethacin-(R)-alpha-ethyl-ethanolamide into cyclooxygenase-1, *Indones. J. Chem.*, 13 (3), 283–286.
- [11] Therneau, T., Atkinson, B., and Ripley, B., 2015, *rpart: Recursive partitioning and regression trees*, R package version 4.1-9, <http://CRAN.R-project.org/package=rpart>.
- [12] Mysinger, M.M., Carchia, M., Irwin, J.J., and Shoichet, B.K., 2012, Directory of useful decoys, enhanced (DUD-E): Better ligands and decoys for better benchmarking, *J. Med. Chem.*, 55 (14), 6582–6594.
- [13] Riswanto, F.D.O., Hariono, M., Yuliani, S.H., and Istyastono, E.P., 2017, Computer-aided design of chalcone derivatives as lead compounds targeting acetylcholinesterase, *Indones. J. Pharm.*, 28 (2), 100–111.
- [14] Yuniarti, N., Mungkasi, S., Yuliani, S.H., and Istyastono, E.P., 2019, Development of a graphical user interface application to identify marginal and potent ligands for estrogen receptor alpha, *Indones. J. Chem.*, 19 (2), 531–537.



- [15] Tosco, P., and Balle, T., 2011, Open3DQSAR: A new open-source software aimed at high-throughput chemometric analysis of molecular interaction fields, *J. Mol. Model.*, 17 (1), 201–208.
- [16] Korb, O., Stützle, T., and Exner, T.E., 2009, Empirical scoring functions for advanced protein-ligand docking with PLANTS, *J. Chem. Inf. Model.*, 49 (1), 84–96.
- [17] Korb, O., Stützle, T., and Exner, T.E., 2007, An ant colony optimization approach to flexible protein-ligand docking, *Swarm Intell.*, 1, 115–134.
- [18] ten Brink, T., and Exner, T.E., 2009, Influence of protonation, tautomeric, and stereoisomeric states on protein-ligand docking results, *J. Chem. Inf. Model.*, 49 (6), 1535–1546.
- [19] O'Boyle, N.M., Banck, M., James, C.A., Morley, C., Vandermeersch, T., and Hutchison, G.R., 2011, Open Babel: An open chemical toolbox, *J. Cheminf.*, 3 (1), 33–47.
- [20] Neudert, G., and Klebe, G., 2011, fconv: Format conversion, manipulation and feature computation of molecular data, *Bioinformatics*, 27 (7), 1021–1022.
- [21] Yuan, S., Chan, H.S., and Hu, Z., 2017, Using PyMOL as a platform for computational drug design, *WIREs Comput. Mol. Sci.*, 7 (2), e1298.
- [22] Krieger, E., and Vriend, G., 2015, New ways to boost molecular dynamics simulations, *J. Comput. Chem.*, 36 (13), 996–1007.
- [23] Liu, K., Watanabe, E., and Kokubo, H., 2017, Exploring the stability of ligand binding modes to proteins by molecular dynamics simulations, *J. Comput. Aided Mol. Des.*, 31 (2), 201–211.